Published in final edited form as:
Neurobiol Dis. 2012 January ; 45(1): 165–176. doi:10.1016/j.nbd.2011.08.001.

Altered Expression of Brain Monocarboxylate Transporter 1 in Models of Temporal Lobe Epilepsy

Fredrik Lauritzen[*,1,5], **Edgar L. Perez**[*,1], **Eric R. Melillo**[1], **Jung-Min Roh**[1], **Hitten P. Zaveri**[2], **Tih-Shih W. Lee**[3], **Yue Wang**[4], **Linda H. Bergersen**[5], and **Tore Eid**[1]

[1]Department of Laboratory Medicine, Yale University School of Medicine, P.O. Box 208035, New Haven, CT 06520, USA

[2]Department of Neurology, Yale University School of Medicine, P.O. Box 208035, New Haven, CT 06520, USA

[3]Department of Psychiatry, Yale University School of Medicine, P.O. Box 208035, New Haven, CT 06520, USA

[4]Department of Neurosurgery, Yale University School of Medicine, P.O. Box 208035, New Haven, CT 06520, USA

[5]The Brain and Muscle Energy Group, Centre for Molecular Biology and Neuroscience and Institute for Basic Medical Sciences, University of Oslo, P.O. Box 1105 Blindern, NO-0317 Oslo, Norway

Abstract

Monocarboxylate transporter 1 (MCT1) facilitates the transport of monocarboxylate fuels (lactate, pyruvate and ketone bodies) and acidic drugs, such as valproic acid, across cell membranes. We recently reported that MCT1 is deficient on microvessels in the epileptogenic hippocampal formation in patients with medication-refractory temporal lobe epilepsy (TLE). To further define the role of MCT1 in the pathophysiology of TLE, we used immunohistochemistry and **stereological analysis** to localize **and quantify** the transporter in the hippocampal formation in three novel and highly relevant rat models of TLE and in nonepileptic control animals. One model utilizes methionine sulfoximine to induce brain glutamine synthetase deficiency and recurrent limbic seizures, while two models employ an episode of perforant pathway stimulation to cause epilepsy. MCT1 was lost on microvessels and upregulated on astrocytes in the hippocampal formation in all models of TLE. Notably, the loss of MCT1 on microvessels was not due to a reduction in microvessel density. The similarities in MCT1 expression among human subjects with TLE and **several** animal models of the disease **strongly** suggest a critical role of this molecule in the pathogenesis of TLE. We hypothesize that the downregulation of MCT1 may promote seizures via impaired uptake of ketone bodies and antiepileptic drugs by the epileptogenic brain. We also propose that the overexpression of MCT1 on astrocytes may lead to increased

Corresponding Authors: Tore Eid, M.D., Ph.D., Department of Laboratory Medicine, Yale University School of Medicine, 333 Cedar Street, P.O. Box 208035, New Haven, CT 06520-8035, USA, Tel: 203-785-4928, Fax: 203-737-2159, tore.eid@yale.edu, Linda H. Bergersen, PhD, Centre for Molecular Biology and Neuroscience, Department of Anatomy and Institute of Basic Medical Sciences, University of Oslo, P.O. Box 1105 Blindern, NO-0317 Oslo, Norway, Tel: +47 22851496, Fax: +47 22851278, l.h.bergersen@medisin.uio.no.
*These authors contributed equally to the work

uptake or release of monocarboxylates by these cells, with important implications for brain metabolism and excitability. These hypotheses can now be rigorously tested in several animal models that replicate key features of human TLE.

Keywords

animal models; blood-brain barrier; glutamine synthetase; hippocampal sclerosis; ketone bodies; ketogenic diet

Introduction

Temporal lobe epilepsy (TLE), which is characterized by spontaneous recurrent seizures that involve limbic brain areas such as the hippocampal formation, remains one of the most common types of medication-refractory epilepsies in humans (Hauser et al., 1993; Spencer, 2002). Even though more than 10 new antiepileptic drugs have been approved for use in the United States since the early 1990s, approximately one-third of all patients with TLE cannot control their seizures despite aggressive pharmacotherapy. More efficacious therapies against TLE are therefore needed, and a better understanding of the mechanism of the disease is likely to facilitate the development of such therapies.

We recently reported that monocarboxylate transporter 1 (MCT1) is deficient on the endothelial cell membrane of microvessels in the epileptogenic hippocampal formation in patients with medication-refractory TLE (Lauritzen et al., 2011). The deficiency is most pronounced in patients with TLE and concomitant hippocampal sclerosis, which is characterized by glial proliferation and loss of neurons, particularly in CA1, CA3 and the dentate hilus of the hippocampal formation (Gloor, 1991; Sommer, 1880). MCT1 facilitates the transport of monocarboxylates, including lactate, pyruvate, acetoacetate and betahydroxybutyrate, across the blood-brain barrier (Bergersen et al., 1999; Cornford et al., 1982; Cremer et al., 1976; Gerhart et al., 1997; Jackson et al., 1995; Koehler-Stec et al., 1998; Leino et al., 1999; Pellerin et al., 1998; Pierre et al., 2000; Price et al., 1998; Terasaki et al., 1991). MCT1 is also a transporter of certain amino acids and acidic drugs, such as valproic acid, between the blood and the brain (Fischer et al., 2008; Kang et al., 1990; Utoguchi and Audus, 2000). Thus, we previously postulated that the uptake of blood-derived monocarboxylate fuels and possibly also antiepileptic drugs is perturbed in the epileptogenic hippocampus in human TLE, due to the loss of MCT1 (Lauritzen et al., 2011). We also proposed that re-expression of MCT1 may represent a novel and highly targeted therapy against medication-refractory TLE.

Carefully controlled studies are required to fully address the possible role of MCT1 in the pathophysiology of TLE. However, because many such studies cannot be readily performed in human subjects, we now seek to explore whether the same perturbations of MCT1 are present in three novel and highly relevant animal models of TLE. One model is based on chronic inhibition of glutamine synthetase in the hippocampal formation (Eid et al., 2008; Wang et al., 2009), while two models utilize electrical stimulation of the perforant pathway to produce recurrent seizures (Bumanglag and Sloviter, 2008; Sloviter, 2008). Compared with the more commonly employed animal models of TLE, such as the paradigms of systemic kainic acid (Ben-Ari, 1985; Nadler and Cuthbertson, 1980) and pilocarpine injections (Turski et al., 1983), the models used here more closely replicate key features of human TLE. For example, the novel models are characterized by (a) an extremely low (<10%) mortality, (b) consistent appearance (>90%) of recurrent seizures that involve limbic brain areas, (c) neuropathological changes that often resemble hippocampal sclerosis and (d) minimal neuronal loss outside limbic brain areas (Bumanglag and Sloviter, 2008; Eid et al.,

2008; Sloviter et al., 2007; Wang et al., 2009). We used immunohistochemistry to study the distribution of MCT1 in the hippocampal formation in the three rat models of TLE. The pattern of MCT1 labeling was also correlated with immunohistochemical markers for blood vessels (RECA-1), astrocytes (GFAP, AQP4) and neurons (MAP, Vglut1).

We hypothesize that MCT1, as in human TLE, is lost on microvessels in the hippocampal formation in all models. If our hypothesis is correct, then several state-of-the-art models of TLE can be used for comprehensive and carefully controlled studies of MCT1 and its role in the pathophysiology of this disease.

Materials and Methods

Chemicals and animals

Chemicals were obtained from Sigma Chemical Co. (St. Louis, Mo.) unless otherwise noted. Male Sprague Dawley rats were used in this study (methionine sulfoximine [MSO] model, 200 to 250 g; perforant pathway stimulation models, 350 to 450 g; Charles River Laboratories, Wilmington, Mass.). Food and water were provided ad libitum. The animal care and use procedures were approved by the Institutional Animal Care and Use Committee of Yale University. All studies were performed in accordance with current guidelines.

MSO model

Chronic infusion of the glutamine synthetase inhibitor MSO unilaterally into the hippocampus in rats leads to recurrent seizures and neuropathological changes similar to those observed in human TLE. The procedure for creating the MSO model is described in detail by (Eid et al., 2008; Wang et al., 2009). Under Isoflurane anesthesia, a drug delivery cannula was introduced into the right hippocampus and connected to a subcutaneously implanted Alzet mini-osmotic pump (Model 2004, Durect Corp., Cupertino, Calif.). In one set of animals, the pump was filled with MSO to achieve a delivery of 0.625 g of MSO per h for ~28 days (as per manufacturer's specifications). In another set, the pump was filled with 0.9% NaCl (saline). The infusion of MSO or saline started immediately postsurgery. Two unipolar **depth** electrodes (E363/2/SPC stainless steel electrode, Plastics One, Roanoke, Va.) with a bare diameter of 0.2 mm and an insulated diameter of 0.23 mm were introduced into the **left and right** dorsal **hippocampal formations** to record **bilateral** intrahippocampal EEG activity. Some animals had two stainless steel screw electrodes (Plastics One) implanted instead of depth electrodes to record EEG activity. This was done to minimize detachment of the electrodes from the animals' skull (see (Wang et al., 2009) for further explanation). The electrodes were positioned in the epidural space overlying the parietal neocortex of each hemisphere. A third electrode was positioned in the epidural space near lambda to serve as the reference. A fourth electrode was positioned over the occipital bone (not touching the dura) to serve as the ground.

Perforant pathway stimulation models

Under Isoflurane anesthesia, rats were implanted bilaterally with two stimulating electrodes (NEX-200 × 3.5 mm, Rhodes Medical Instruments, Summerland, Calif.) and two **custom made tungsten** recording electrodes with a bare diameter of 0.076 mm and an insulated diameter of 0.11 mm (A-M Systems, Carlsborg, Wash.). The electrodes were placed in the angular bundle of the perforant pathway and **in the** dentate granule cell layer, respectively, as previously described (Harvey and Sloviter, 2005). The optimal locations of the stimulating electrodes were determined by maximizing the evoked responses to perforant pathway stimulation (Andersen et al., 1966). Two screws serving as ground and reference **electrodes** were positioned anterior to the bregma, one over each hemisphere. The female socket contacts on the ends of the electrodes were inserted into two plastic pedestals

(Plastics One), and the entire setup was secured by UV curing acrylic adhesive (Loctite 3106 light cure adhesive, Henkel Loctite Corp., Rocky Hill, **Conn**.).

At least two weeks postsurgery, awake animals were stimulated bilaterally for 3 or 8 h. In the 3-h paradigm, 15- to 20-V paired-pulse stimuli were delivered at 2 Hz, with a 40-ms interpulse interval. These stimuli were coupled with 10-s-long 20-Hz stimulus trains of single 15- to 20-V stimuli delivered every minute. In the 8-h paradigm, 10-s-long 20-Hz stimulus trains of single 30-V stimuli with 0.1-ms duration were delivered once per minute. These paradigms are designed to evoke hippocampal granule and pyramidal cell discharges (Sloviter et al., 1996). Isoflurane gas was administered to the rats at the end of the 3- or 8-h stimulation paradigms to terminate residual seizure activity. Rats appeared to be fully recovered behaviorally and resumed normal eating and drinking habits approximately one day after stimulation.

Video-intracranial EEG monitoring

The experimental setup for recording video-EEG was adapted from the work of Bertram et al. (Bertram et al., 1997). The rats were housed individually in custom-made Plexiglas cages, and video-intracranial EEG monitoring was initiated immediately after stimulation **or after the onset of MSO or saline infusion**. A spring-covered, 6-channel cable connected the electrode pedestal to a commutator (Plastics One), while a second cable connected the commutator to the digital EEG recording unit (Ceegraph VISION LTM, Natus Medical, Mundelein, Ill.). Digital cameras with infrared capacity were used to record animal behavior. The digital video signal was encoded and synchronized to the digital EEG signals. Seizures were identified by visual inspection of the EEG record. Interictal activity is essentially transient in nature and can be distinguished by its duration; subclinical seizures can be distinguished by examination of the video record. To establish the start and stop points of a seizure, we determined a point that was unequivocally within the seizure and moved backward and forward in time to the points where the EEG was characterized by normal baseline activity. The video record was examined to score the seizures on a modified Racine scale (Racine et al., 1973) as follows: Subclinical, no remarkable behavior; Stage I, immobilization, eye blinking, twitching of vibrissae and mouth movements; Stage II, head nodding, often accompanied by facial clonus; Stage III, forelimb clonus; Stage IV, rearing; Stage V, rearing, falling and generalized convulsions. Recurrent seizures were defined as ≥2 seizures of Stage III or higher at least 1 h apart.

Tissue preparation

After continuous video-EEG recordings for several days, the rats were reanesthetized and perfused transcardially either with saline followed by 4% paraformaldehyde (PFA)-0.1% glutaraldehyde in phosphate buffer (PB; 0.1 M, pH 7.4) (perforant pathway stimulation groups) or with saline followed by 4% PFA in PB (MSO group). In the MSO group, the brains were subsequently removed, postfixed in the same solution overnight at 4°C and stored at −80°C. In the perforant pathway stimulation groups, the brains were left in situ for 4 h at 4°C before being removed from the skulls. A Vibratome and sliding microtome were used to cut 80-μm- and 50-μm-thick brain sections from the MSO and perforant pathway stimulation models, respectively. Every fifth section was transferred to a gelatin-coated slide and stained with cresyl violet. Subsets of the remaining sections were used for immunohistochemistry.

Immunohistochemistry

For single-labeling immunohistochemistry, sections from the MSO model and perforant pathway stimulation models were incubated free-floating in **solutions** of chicken anti-MCT1 antibody (AB1286, Millipore, Billerica, Mass.) diluted 1:10,000 (MSO model) or 1:1,000

(perforant pathway stimulation models), or mouse anti-RECA-1 antibody (MCA970R, AbD Serotec, Dusseldorf, Germany) diluted 1:1,000. All antibodies were incubated with tissue sections for 72 h at 4°C and processed according to the avidin biotin peroxidase method (Hsu et al., 1981), using the Vectastain Elite Kit (Vector Laboratories, Burlingame, Calif.) with diaminobenzidine as the chromogen. Sections labeled with RECA-1 were counterstained with cresyl violet. The immunostained sections were mounted on gelatin-coated glass slides, cover-slipped and examined by light microscopy. For double-labeling fluorescence immunohistochemistry, Vibratome sections were incubated at room temperature for 24 h (20 to 24°C), free-floating in a mixture of chicken anti-MCT1 (1:1,000) and either mouse anti-RECA-1 (1:2,500), mouse anti-GFAP (MAB360, Millipore; 1:2,000), rabbit anti-AQP4 (AB3594, Millipore; 1:2,000), rabbit anti-synaptophysin 1 (101002, Synaptic Systems, Goettingen, Germany; 1:500), rabbit anti-Vglut1 (135302, Synaptic Systems; 1:10,000), mouse anti-PSD95 (MAB1598, Millipore; 1:1,000) or mouse anti-MAP 2A/2B (MAB378, Millipore; 1:1,500). After washing, sections were incubated for 2 h in a mixture of Alexa Fluor 488 goat anti-chicken IgG and either Alexa Fluor 555 goat anti-mouse IgG or Alexa Fluor 633 goat anti-rabbit IgG. All fluorescent secondary antibodies were diluted 1:1,000. Double-labeled sections were examined by a confocal laser-scanning microscope (Zeiss LSM META, Carl Zeiss MicroImaging, Thornwood, N.Y.).

To quantify the density of microvessels labeled with MCT1 or RECA-1 in the hippocampal formation, stereological point count analysis was carried out (Gundersen, 1988). Hippocampal formations from MSO-infused (MSO R, n=6 and n=5), contralateral untreated hippocampal formations of MSO-infused rats (MSO L, n=6 and n= 6), saline infused (n=6 and n=6), sham-operated (n=5 and n=4), 3h-stimulated (n=9, n=9) and 8h-stimulated (n=4 and n=4) rats were included in the analysis of MCT1 and RECA-1 respectively. The densities of MCT1 or RECA-1 positive microvessels in each hippocampal formation, i.e. an area comprising of the dentate gyrus, the dentate hilus, CA3, CA2, CA1 and subiculum, were calculated by the following procedure. (1) One image of the dorsal part of the hippocampal formation was taken from each rat using a light microscope. (2) A test system with a set of regularly spaced points was superimposed on to each image. (3) Points hitting MCT1-, or RECA-1 positive structures within the hippocampal formation were counted and divided by the total number of points within the hippocampal profile. The investigator performing the counts was blinded to the experimental identity of the tissue. The density of blood vessels was expressed as number of counts hitting the blood vessels per 100 total counts.

Statistical Analysis

Analysis of repeated measurements was performed using a one way ANOVA with a Tukey-Kramer multiple comparisons post test. The significance level was set to a P value of <0.05. Unless otherwise noted, the data are presented as mean ± standard deviation.

Results

Nissl stain

Using Nissl-stained tissue sections, we first assessed the general histopathology of the hippocampal formations from each of the five groups of rats included in this study (Fig. 1). Animals continuously infused with saline into the right hippocampal formation (MSO control group; $n = 6$) displayed either a narrow zone of neuronal loss and gliosis around the saline infusion cannula or no significant neuronal loss or gliosis in the hippocampal formation (Fig. 1A1-4). Five of the six animals continuously infused with MSO into the right hippocampal formation ($n = 6$) did not exhibit significant neuronal loss or glial proliferation in the left contralateral hippocampal formation (Fig. 1B1-4), whereas all MSO-

treated animals exhibited a range of morphological changes in the right hippocampal formation, from minimal to significant neuronal loss and including a sclerosis-like pathology (Fig. 1C1-4), as previously reported (Eid et al., 2008; Wang et al., 2009). One MSO-treated rat had glial proliferation and moderate loss of pyramidal neurons in CA3 of the contralateral (left) **untreated** hippocampus (not shown). Sham-operated, nonstimulated rats (perforant pathway stimulation control group; $n = 5$) did not exhibit significant neuronal loss or proliferation of glial cells in the hippocampal formation (Fig. 1D1-4). Rats subject to perforant pathway stimulation for 3 h ($n = 10$, Fig. 1E1-4) or 8 h ($n = 5$, Fig. 1F1-4) exhibited a range of neuropathological changes. The changes in the 3-h stimulation group were distributed as follows: (a) no **visual** neuronal loss or gliosis (3 of 10 rats), (b) neuronal loss and gliosis mainly in the hilus (1 of 10 rats), (c) neuronal loss and gliosis in the hilus and CA3 (2 of 10 rats) and (d) hippocampal sclerosis (4 of 10 rats) (Fig. 1E1-4). Eight hours of perforant pathway stimulation resulted in a hippocampal sclerosis-like picture in 4 of 5 rats (Fig 1F1-4) and 1 rat with extensive neuronal loss throughout the hippocampal formation. Two 8-h-stimulated rats with hippocampal sclerosis also experienced a moderate loss of the dentate granule cells (data not shown).

Continuous video-intracranial EEG monitoring

All rats were monitored by video-intracranial EEG for continuous periods up to a maximum of 73 days. None of the saline-infused ($n = 6$) or sham-operated, nonstimulated ($n = 5$) rats exhibited recurrent seizures (Fig. 2A). In contrast, all of the MSO-treated ($n = 6$, Fig. 2B) and 8-h-stimulated ($n = 5$, Fig. 2D) rats developed recurrent seizures. All but one 3-h stimulated rat ($n = 10$) had recurrent seizures (Fig. 2C). This rat's electrode implantation fell off on the third day of recording. Had it stayed on for a longer period, we probably would have captured recurrent seizures in this animal as well.

MCT1 immunohistochemistry

A widespread network of MCT1-positive blood vessels was present in the hippocampal formation in the saline-infused rats (Fig. 3A1-4), nonstimulated controls (Fig. 3D1-4) and left (noninfused) hippocampal formation in the MSO-treated animals (Fig. 3B1-4). In contrast, markedly fewer MCT1-immunoreactive blood vessels were present in the right hippocampal formation in the MSO-infused rats (Fig. 3C1-4) and in both hippocampal formations in the two stimulation models (Fig. 3E, F). Specifically, MCT1 was lost on microvessels in the dentate hilus in all of the epileptic rats, independent of the model studied (Fig. $3C_2$, E_2, F_2). MCT1 was also lost on microvessels in CA3 and CA1 in MSO-treated (Fig. $3C_{3,4}$;) and electrically stimulated rats (Fig. $3E_{3,4}$ and $3F_{3,4}$). A large number of the epileptic rats, but none of the control animals, also revealed areas of increased MCT1 immunoreactivity in the hippocampal formation. The increased immunoreactivity was distributed diffusely in a granular pattern in the hilus, CA3 and CA1 in 85% of the MSO-treated animals (Fig. 3C), 70% of the 3-h-stimulated animals (Fig. 3E) and all of the 8-h-stimulated animals (Fig. 3F).

A comprehensive quantitative analysis revealed no significant difference in the density of MCT1-positive blood vessels between the right saline-treated hippocampal formation and the left (untreated) hippocampal formation in the MSO-infused rats (Fig. 4A). In contrast, the density of MCT1-positive microvessels was reduced by approximately 70 % in the right MSO-infused hippocampal formation vs. the left (untreated) hippocampal formation in the same animals and vs. the hippocampal formation in the saline treated controls (Fig. 4A). The density of MCT1-positive microvessels was reduced by approximately 80% in the hippocampal formation in the 3h and 8h stimulated rats vs. the non-stimulated control rats (Fig. 4B).

RECA-1 immunohistochemistry

We next analyzed the density of blood vessels in the hippocampal formations in all animals using the endothelial cell marker RECA-1. This was done to assess whether the loss of MCT1 on microvessels in TLE is merely due to a reduced vascular density in this disease. Visual evaluations of the RECA-1 positive blood vessels revealed dense networks of blood vessels in all subfields of the hippocampal formation in all animal groups (Fig. 5A-F). Quantitative analysis revealed no difference in blood vessel densities among hippocampal formations in the saline/MSO groups (Fig. 5G, $P = 0.147$) and in the sham/stimulated groups (Fig. 5H, $P = 0.961$). As expected, the ratio of MCT1 to RECA-1 labeling tended to be lower for MSO R, 3h and 8h-stim compared to in saline, MSO L and Sham-control (Fig. 5I).

Double-labeling confocal microscopy

To further assess the cellular localization of MCT1 in the hippocampal formations of the epileptic animals, double-labeling experiments were performed using MCT1 and one of the following markers for, astrocytes (GFAP, Fig. 6A; AQP4, Fig. 6B) or neurons (MAP 2A/2B, Vglut1, synaptophysin 1 or PSD95, Fig. 6C, D). Because the different epilepsy models showed similar patterns of MCT1 labeling, the study was limited to analysis of 8-h-stimulated rats and sham-operated controls. In the hippocampal formations in non-stimulated control rats, MCT1 was predominantly found on circular structures (Fig. $6A_1$, B_1, C_1, D_1) which co-localized with the endothelial cell marker RECA-1 (not shown), confirming that MCT1 is mainly localized to endothelial cells under normal conditions. Only minimal labeling for MCT1 was present on non-endothelial cells in non-stimuated control rats (Fig. 6A-D). While MCT1 did not co-localize with GFAP in hippocampal formations in control rats (Fig. $6A_{1\text{-}3}$), such co-localization was strikingly present in epileptic animals (Fig. $6A_{4\text{-}6}$). The overall density of GFAP labeling was also greatly increased in neuron-depleted (sclerotic) areas of the hippocampal formation in epileptic animals (Fig. $6A_{5,6}$) vs. the same areas in controls (Fig. $6A_{2,3}$). In the epileptic animals, GFAP not only labeled discrete bundles of astrocyte filaments but also often labeled the entire cytoplasm of cells. Such diffuse cytoplasmic labeling with GFAP was not seen in control animals.

Although MCT1 was located near AQP4 in control animals, the two molecules did not completely overlap (Fig. $6B_{1\text{-}3}$). The lack of overlap can be explained by the fact that, under normal conditions, MCT1 preferentially labels endothelial cells, whereas AQP4 primarily labels perivascular astrocyte endfeet (Eid et al., 2005; Frigeri et al., 1995; Lauritzen et al., 2011; Lee et al., 2004a; Nielsen et al., 1997). However, in the hippocampal formation in epileptic rats, increased labeling for AQP4 was present in the extravascular neuropil relative to the perivascular compartment (Fig. $6B_{5,6}$). Such increase in extravascular AQP4 is also present in human TLE (Eid et al., 2005; Lee et al., 2004b). In the hippocampal formation in epileptic rats, extravascular MCT1 showed pronounced overlap with AQP4 (Fig. $6B_{4\text{-}6}$), whereas such overlap was not seen in control rats (Fig. $6B_{1\text{-}3}$). This observation indicates that MCT1 is strongly expressed on the plasma membrane of astrocytes in the extravascular neuropil in the epileptogenic hippocampal formation.

Finally, an assessment of MCT1 and a variety of neuronal markers did not reveal any colocalization between MCT1 and MAP 2A/2B (Fig. $6C_{1,2}$), Vglut1 (Fig. $6D_{1,2}$), synaptophysin 1 (not shown) or PSD95 (not shown) in the hippocampal formation in epileptic or control rats.

Discussion

Due to the intriguing observation that the density of MCT1 is greatly reduced on microvessels in the hippocampal formation in human TLE (Lauritzen et al., 2011), we hypothesized that a similar loss of MCT1 would be present in relevant animal models of the disease. We have now shown that MCT1 is indeed deficient on the endothelial cell membrane of microvessels in the hippocampal formation in three newly developed rat models of TLE. Moreover, this deficiency is not due to a loss of brain microvessels. We have also demonstrated that the loss of MCT1 on microvessels is accompanied by an overexpression of the transporter on astrocytes in the neuropil. The potential relevance of these findings will be discussed below.

Loss of MCT1 on brain microvessels

A deficiency in MCT1 on microvessels in the hippocampal formation in TLE was first reported in patients undergoing resection of the anteromedial temporal lobe for the treatment of medication-refractory TLE (Lauritzen et al., 2011). In this patient population, MCT1 was severely deficient on the endothelial cell membrane of microvessels in several areas of the hippocampal formation, especially CA1, but also CA3 and the hilus of the dentate gyrus. The loss of microvessel-associated MCT1 was most prominent in TLE patients with concomitant hippocampal sclerosis, although a smaller reduction in MCT1 was also evident in TLE patients without hippocampal sclerosis compared with that in autopsy specimens from nonepileptic control subjects. The observation that MCT1 is lost on brain microvessels in human TLE as well as in three different animal models of the disease indicates that a lack of MCT1 on microvessels is of critical importance for the pathophysiology of the disease.

MCT1 is a key carrier molecule for monocarboxylates, amino acids and acidic drugs across the blood-brain barrier, and a deficiency in MCT1 is expected to impair the uptake of such compounds by the brain. The potential significance of such impaired uptake has been discussed in detail in our previous paper on the loss of MCT1 in human TLE (Lauritzen et al., 2011); thus, only a brief summary of the most pertinent points of this discussion will be provided here.

Firstly, the loss of MCT1 may result in decreased concentrations of blood-derived monocarboxylate fuels, especially ketone bodies, in the epileptogenic hippocampus. The presence of ketone bodies in the brain has been proposed to increase the brain energy stores (Pan et al., 1999), stabilize the neuronal membrane potential (Bough, 2008), enhance GABA-mediated inhibition (Cantello et al., 2007; Yudkoff et al., 2004), inhibit the transport of glutamate into synaptic vesicles (Juge et al., 2010) and attenuate the release of vesicular glutamate by neurons (Juge et al., 2010). Low basal levels of brain ketone bodies may therefore contribute to the seizure susceptibility of the hippocampal formation in TLE. Furthermore, treatment with a high-fat, low-carbohydrate – i.e., ketogenic – diet may reverse the deleterious effects of the MCT1 deficiency by enhancing the uptake of ketone bodies via existing MCT1 due to an increased concentration gradient between the blood and the brain, or by induction of the synthesis of additional MCT1 on brain microvessels, as demonstrated by Leino and colleagues (Leino et al., 2001).

Secondly, because the transport of acidic drugs such as valproic acid across the blood-brain barrier is facilitated by MCT1 (Fischer et al., 2008; Kang et al., 1990; Utoguchi and Audus, 2000), the tissue concentration of key antiepileptic drugs may be remarkably low in the MCT1-deficient, epileptogenic hippocampus. Some patients with TLE are resistant to valproic acid and other antiepileptic drugs, and the lack of MCT1 represents an attractive possible explanation for such pharmacoresistance.

Thirdly, the loss of MCT1 on brain microvessels in TLE may be accompanied by a concomitant upregulation of multidrug-resistance-associated proteins (MDPs) on the same blood vessels (Aronica et al., 2004; Kubota et al., 2006). MDPs facilitate the efflux of antiepileptic drugs from brain tissue, and a combination of decreased MCT1 and increased MDPs is expected to effectively prevent accumulation of antiepileptic drugs to therapeutic levels in the epileptogenic hippocampus (Cascorbi, 2010; Loscher, 2007; Marchi et al., 2010).

Overexpression of MCT1 on astrocytes

The second major finding, that MCT1 is overexpressed on astrocytes in the hippocampal neuropil in the three models of TLE, is also likely to be true for the epileptogenic hippocampal formation in human TLE. We previously reported a pattern of diffuse labeling with MCT1 in the neuropil of the hippocampal formation in patients with TLE and concomitant hippocampal sclerosis (Lauritzen et al., 2011). Such labeling was most prominent in areas of neuronal loss and astroglial proliferation such as the CA1. Although double-labeling experiments with MCT1 and astroglial markers were not performed in this study, the labeling pattern is strikingly similar to what we have now identified as an overexpression of MCT1 on astrocytes. A key question is whether the overexpression of MCT1 on astrocytes indicates increased efflux or influx of monocarboxylates in these cells.

Several arguments support the hypothesis that the overexpression of MCT1 causes enhanced efflux of monocarboxylates from astrocytes. Due to the increased release of extracellular glutamate during seizures (During and Spencer, 1993), the clearance of the neurotransmitter by astrocytes is likely to be enhanced. Because the cellular uptake of glutamate by glutamate transporters is energy-dependent (reviewed by (Danbolt, 2001), more ATP is required during conditions of excessive glutamate uptake. A highly active glycolytic pathway, which is an important source of ATP in astrocytes (Bergersen, 2007; Hertz and Dienel, 2005; Pellerin and Magistretti, 2003), will result in large amounts of lactate and protons, which must be removed from the cytosol to continue the synthesis of ATP. An increased expression of MCT1 on astrocytes could therefore boost the efflux of lactate and protons from these cells. The lactate efflux hypothesis presented here is also supported by the observation in human TLE that the interictal (basal) extracellular concentration of lactate is approximately 48% higher in the epileptogenic hippocampal formation (6.8 mM) than in the nonepileptogenic hippocampal formation (4.6 mM) (Cavus et al., 2005) and 90% higher during, and in the first hour (60 to 90 min) after, spontaneous complex partial seizures with secondary generalization (During et al., 1994). The biological effects of high extracellular brain lactate are not clearly understood, but one possibility is that increased lactate levels lead to decreased pH in the epileptic focus with arrest of seizure activity and postictal refractoriness. The antiseizure effect of low pH is probably mediated by reduced currents through the n-methyl-D-aspartate (NMDA) receptor (During et al., 1994).

It can also be argued that the upregulation of astrocytic MCT1 facilitates an increased influx of monocarboxylates into these cells, due to alterations in the astrocyte metabolism. Such upregulation of MCT1 is evident in skeletal muscle cells when the metabolism changes from glycolytic to oxidative after experimental reinnervation by a nerve that causes a continuous activation pattern (Bergersen et al., 2006). Hosoi and colleagues have shown that the monocarboxylate acetate is taken up by cultured rat astrocytes via MCT1 and that the uptake is enhanced when glutamate is added to the medium (Hosoi et al., 2009). The same group also discovered a 130 to 240% increase in the brain uptake of acetate 2 h after systemic injection of the chemoconvulsant pilocarpine (Hosoi et al., 2010). Thus, increased flux of monocarboxylates into astrocytes is likely to occur during glutamate stimulation and seizures. The upregulation of MCT1 on astrocytes in TLE may therefore reflect an increased

metabolic demand for acetate and other monocarboxylates in epileptogenic areas of the brain.

Finally, the overexpression of MCT1 on astrocytes also suggests a lactate “siphoning” potential of the astrocyte syncytium in TLE. For example, neurons can release lactate into the extracellular space during periods of excitation and high glycolytic activity (Dienel and Cruz, 2008). The released lactate may then be taken up by perisynaptic astrocytes via MCT1 and “siphoned” via the astrocytic syncytium away from regions of high neuronal activity and toward areas of lower activity where the lactate can be more effectively metabolized. The lactate taken up this way may also be “siphoned” toward blood vessels and released to the blood for metabolism by peripheral organs such as liver, heart and oxidative skeletal muscle fibers; however, such a scenario is less likely in the hippocampal formation in TLE, where MCT1 is deficient on endothelial cells.

Conclusions

The observation that MCT1 is deficient on microvessels and overexpressed on astrocytes in the hippocampal formation in three relevant animal models of TLE and also in humans with the disease raises the possibility that MCT1 is critically involved in the pathophysiology of TLE. We hypothesize that the downregulation of vascular MCT1 may promote seizures via impaired uptake of ketone bodies and antiepileptic drugs by the epileptogenic brain. We also propose that the overexpression of MCT1 on astrocytes may lead to increased uptake or release of lactate, protons or other monocarboxylates by these cells, with important implications for brain metabolism and excitability. Finally, we suggest that pharmaceutical manipulation of MCT1 in patients with medication-refractory TLE may represent a novel, selective and efficacious therapeutic strategy for the disease. Carefully controlled studies using the animal models presented here are in progress to further define the role of MCT1 in TLE and to specifically address the hypotheses stated above.

Acknowledgments

We thank Ms. Ilona Kovacs for excellent technical assistance, Ms. Anne Sommer for editorial advice, and Dr. Robert Sloviter for advice on the use of the perforant pathway stimulation models. This work was supported by grants from the National Institutes of Health (NIH) NS058674 (to T.E.), The Swebelius Foundation, the Medical Faculty of the University of Oslo (to F.L.) and the Research Council of Norway (to F.L. and L.H.B.). Part of this work was also made possible by Clinical and Translational Science Award (CTSA) grant UL1 RR024139 from the National Center for Research Resources (NCRR), a component of the NIH, and by the NIH Roadmap for Medical Research. Its contents are solely the responsibility of the authors and do not necessarily represent the official view of NCRR or NIH.

References

Andersen P, et al. Entorhinal activation of dentate granule cells. Acta Physiol Scand. 1966; 66:448–60. [PubMed: 5927271]

Aronica E, et al. Expression and cellular distribution of multidrug resistance-related proteins in the hippocampus of patients with mesial temporal lobe epilepsy. Epilepsia. 2004; 45:441–51. [PubMed: 15101825]

Ben-Ari Y. Limbic seizure and brain damage produced by kainic acid: mechanisms and relevance to human temporal lobe epilepsy. Neuroscience. 1985; 14:375–403. [PubMed: 2859548]

Bergersen L, et al. Cellular and subcellular expression of monocarboxylate transporters in the pigment epithelium and retina of the rat. Neuroscience. 1999; 90:319–331. [PubMed: 10188957]

Bergersen LH. Is lactate food for neurons? Comparison of monocarboxylate transporter subtypes in brain and muscle. Neuroscience. 2007; 145:11–9. [PubMed: 17218064]

Bergersen LH, et al. Cross-reinnervation changes the expression patterns of the monocarboxylate transporters 1 and 4: An experimental study in slow and fast rat skeletal muscle. Neuroscience. 2006; 138:1105–13. [PubMed: 16446038]

Bertram EH, et al. Design and construction of a long-term continuous video-EEG monitoring unit for simultaneous recording of multiple small animals. Brain Res. Brain Res. Protoc. 1997; 1997:85–97. [PubMed: 9438076]

Bough K. Energy metabolism as part of the anticonvulsant mechanism of the ketogenic diet. Epilepsia. 2008; 49(Suppl 8):91–3. [PubMed: 19049599]

Bumanglag AV, Sloviter RS. Minimal latency to hippocampal epileptogenesis and clinical epilepsy after perforant pathway stimulation-induced status epilepticus in awake rats. J Comp Neurol. 2008; 510:561–80. [PubMed: 18697194]

Cantello R, et al. Ketogenic diet: electrophysiological effects on the normal human cortex. Epilepsia. 2007; 48:1756–63. [PubMed: 17561954]

Cascorbi I. ABC transporters in drug-refractory epilepsy: limited clinical significance of pharmacogenetics? Clin Pharmacol Ther. 2010; 87:15–8. [PubMed: 20019695]

Cavus I, et al. Extracellular metabolites in the cortex and hippocampus of epileptic patients. Ann Neurol. 2005; 57:226–35. [PubMed: 15668975]

Cornford EM, et al. Developmental modulations of blood-brain barrier permeability as an indicator of changing nutritional requirements in the brain. Pediatr Res. 1982; 16:324–8. [PubMed: 7079003]

Cremer JE, et al. Changes during development in transport processes of the blood-brain barrier. Biochim Biophys Acta. 1976; 448:633–7. [PubMed: 823975]

Danbolt NC. Glutamate uptake. Prog. Neurobiol. 2001; 65:1–105. [PubMed: 11369436]

Dienel GA, Cruz NF. Imaging brain activation: simple pictures of complex biology. Ann N Y Acad Sci. 2008; 1147:139–70. [PubMed: 19076439]

During MJ, et al. Direct measurement of extracellular lactate in the human hippocampus during spontaneous seizures. J Neurochem. 1994; 62:2356–61. [PubMed: 8189240]

During MJ, Spencer DD. Extracellular hippocampal glutamate and spontaneous seizure in the conscious human brain. Lancet. 1993; 341:1607–10. [PubMed: 8099987]

Eid T, et al. Recurrent seizures and brain pathology after inhibition of glutamine synthetase in the hippocampus in rats. Brain. 2008; 131:2061–70. [PubMed: 18669513]

Eid T, et al. Loss of perivascular aquaporin 4 may underlie deficient water and K+ homeostasis in the human epileptogenic hippocampus. Proc Natl Acad Sci U S A. 2005; 102:1193–8. [PubMed: 15657133]

Fischer W, et al. Transport of valproate at intestinal epithelial (Caco-2) and brain endothelial (RBE4) cells: mechanism and substrate specificity. Eur J Pharm Biopharm. 2008; 70:486–92. [PubMed: 18577448]

Frigeri A, et al. Immunolocalization of the mercurial-insensitive water channel and glycerol intrinsic protein in epithelial cell plasma membranes. Proc Natl Acad Sci U S A. 1995; 92:4328–31. [PubMed: 7538665]

Gerhart DZ, et al. Expression of monocarboxylate tranpsorter MCT1 by brain endothelium and glia in adult and suckling rats. Am J Physiol. 1997; 273:207–213.

Gloor, P. Mesial temporal sclerosis: Historical background and an overview from a modern perspective. In: Luders, H., editor. Epilepsy Surgery. Raven Press; New York: 1991. p. 6889-703.

Gundersen, H. J. G. e. a. The new stereological tools. APMIS. 1988; 96:379–394. 857–881. [PubMed: 3288247]

Harvey BD, Sloviter RS. Hippocampal granule cell activity and c-Fos expression during spontaneous seizures in awake, chronically epileptic, pilocarpine-treated rats: implications for hippocampal epileptogenesis. J Comp Neurol. 2005; 488:442–63. [PubMed: 15973680]

Hauser WA, et al. Incidence of epilepsy and unprovoked seizures in Rochester, Minnesota: 1935-1984. Epilepsia. 1993; 34:453–68. [PubMed: 8504780]

Hertz L, Dienel GA. Lactate transport and transporters: general principles and functional roles in brain cells. J Neurosci Res. 2005; 79:11–8. [PubMed: 15586354]

Hosoi R, et al. Remarkable increase in 14C-acetate uptake in an epilepsy model rat brain induced by lithium-pilocarpine. Brain Res. 2010; 1311:158–65. [PubMed: 19909730]

Hosoi R, et al. Characterization of (14)C-acetate uptake in cultured rat astrocytes. Brain Res. 2009; 1253:69–73. [PubMed: 19073161]

Hsu S, et al. Use of avidin-biotin-peroxidase complex (ABC) in immunoperoxidase techniques: a comparison between ABC and unlabeled antibody (PAP) procedures. J. Histochem. Cytochem. 1981; 29:577–580. [PubMed: 6166661]

Jackson VN, et al. cDNA cloning of MCT1, a monocarboxylate transporter from rat skeletal muscle. Biochim Biophys Acta. 1995; 1238:193–6. [PubMed: 7548134]

Juge N, et al. Metabolic control of vesicular glutamate transport and release. Neuron. 2010; 68:99–112. [PubMed: 20920794]

Kang YS, et al. Acidic drug transport in vivo through the blood-brain barrier. A role of the transport carrier for monocarboxylic acids. J Pharmacobiodyn. 1990; 13:158–63. [PubMed: 2117062]

Koehler-Stec EM, et al. Monocarboxylate ransporter expression in mouse brain. Am J Physiol. 1998; 275:E516–E524. [PubMed: 9725820]

Kubota H, et al. Distribution and functional activity of P-glycoprotein and multidrug resistance-associated proteins in human brain microvascular endothelial cells in hippocampal sclerosis. Epilepsy Res. 2006; 68:213–28. [PubMed: 16361082]

Lauritzen F, et al. Monocarboxylate transporter 1 is deficient on microvessels in the human epileptogenic hippocampus. Neurobiol Dis. 2011; 41:577–84. [PubMed: 21081165]

Lee TS, et al. Aquaporin-4 is increased in the sclerotic hippocampus in human temporal lobe epilepsy. Acta Neuropathol (Berl). 2004a; 108:493–502. [PubMed: 15517312]

Lee TS, et al. Aquaporin-4 is increased in the sclerotic hippocampus in human temporal lobe epilepsy. Acta Neuropathol (Berl). 2004b

Leino RL, et al. Monocarboxylate transporter (MCT1) abundance in brains of suckling and adult rats: a quantitative electron microscopic immunogold study. Brain Res Dev Brain Res. 1999; 113:47–54.

Leino RL, et al. Diet-induced ketosis increases monocarboxylate transporter (MCT1) levels in rat brain. Neurochem. Int. 2001; 38:519–527. [PubMed: 11248400]

Loscher W. Drug transporters in the epileptic brain. Epilepsia. 2007; 48(Suppl 1):8–13. [PubMed: 17316407]

Marchi N, et al. Transporters in drug-refractory epilepsy: clinical significance. Clin Pharmacol Ther. 2010; 87:13–5. [PubMed: 20019694]

Nadler J, Cuthbertson G. Kainic acid neurotoxicity toward the hippocampal formation: dependence on specific excitatory pathways. Brain Res. 1980; 195:47–56. [PubMed: 6249441]

Nielsen S, et al. Specialized membrane domains for water transport in glial cells: high-resolution immunogold cytochemistry of aquaporin-4 in rat brain. J Neurosci. 1997; 17:171–80. [PubMed: 8987746]

Pan JW, et al. Ketosis and epilepsy: 31P spectroscopic imaging at 4.1 T. Epilepsia. 1999; 40:703–7. [PubMed: 10368066]

Pellerin L, Magistretti PJ. Food for thought: challenging the dogmas. J Cereb Blood Flow Metab. 2003; 23:1282–6. [PubMed: 14600434]

Pellerin L, et al. Expression of monocarboxylate transporter mRNAs in mouse brain: support for a distinct role of lactate as an energy substrate for the neonatal vs. adult brain. Proc Natl Acad Sci U S A. 1998; 95:3990–5. [PubMed: 9520480]

Pierre K, et al. Cell-specific localization of monocarboxylate transporters, MCT1 and MCT2, in the adult mouse brain revealed by double immunohistochemical labeling and confocal microscopy. Neuroscience. 2000; 100:617–27. [PubMed: 11098125]

Price NT, et al. Cloning and sequencing of four new mammalian monocarboxylate transporter (MCT) homologues confirms the existence of a transporter family with an ancient past. Biochem J. 1998; 329(Pt 2):321–8. [PubMed: 9425115]

Racine RJ, et al. Rates of motor seizure development in rats subjected to electrical brain stimulation: strain and inter-stimulation interval effects. Electroencephalogr Clin Neurophysiol. 1973; 35:553–6. [PubMed: 4126463]

Sloviter RS. Hippocampal epileptogenesis in animal models of mesial temporal lobe epilepsy with hippocampal sclerosis: the importance of the “latent period” and other concepts. Epilepsia. 2008; 49(Suppl 9):85–92. [PubMed: 19087122]

Sloviter RS, et al. Basal expression and induction of glutamate decarboxylase and GABA in excitatory granule cells of the rat and monkey hippocampal dentate gyrus. J Comp Neurol. 1996; 373:593–618. [PubMed: 8889946]

Sloviter RS, et al. On the relevance of prolonged convulsive status epilepticus in animals to the etiology and neurobiology of human temporal lobe epilepsy. Epilepsia. 2007; 48(Suppl 8):6–10. [PubMed: 18329985]

Sommer W. Erkrankung des Ammonshorns als aetiologisches Moment der Epilepsie. Arch. Psychiatr. Nervenkr. 1880; 10:631–675.

Spencer SS. Neural networks in human epilepsy: evidence of and implications for treatment. Epilepsia. 2002; 43:219–27. [PubMed: 11906505]

Terasaki T, et al. Transport of monocarboxylic acids at the blood-brain barrier: studies with monolayers of primary cultured bovine brain capillary endothelial cells. J Pharmacol Exp Ther. 1991; 258:932–7. [PubMed: 1890627]

Turski WA, et al. Limbic seizures produced by pilocarpine in rats: behavioural, electroencephalographic and neuropathological study. Behav Brain Res. 1983; 9:315–35. [PubMed: 6639740]

Utoguchi N, Audus KL. Carrier-mediated transport of valproic acid in BeWo cells, a human trophoblast cell line. Int J Pharm. 2000; 195:115–24. [PubMed: 10675689]

Wang Y, et al. The development of recurrent seizures after continuous intrahippocampal infusion of methionine sulfoximine in rats: a video-intracranial electroencephalographic study. Exp Neurol. 2009; 220:293–302. [PubMed: 19747915]

Yudkoff M, et al. Ketogenic diet, brain glutamate metabolism and seizure control. Prostaglandins Leukot Essent Fatty Acids. 2004; 70:277–85. [PubMed: 14769486]

Research Highlights

- Alterations in brain MCT1 are present in human temporal lobe epilepsy (TLE)
- Similar alterations have now been found in three animal models of TLE
- These findings suggest a key role of MCT1 in the pathophysiology of TLE
- The exact role of MCT1 in TLE can now be tested in relevant animal models

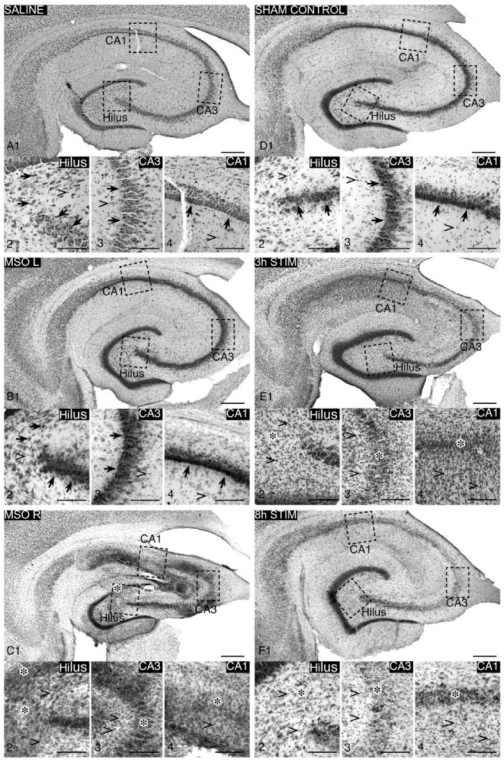

Fig. 1.

Nissl-stained horizontal sections of hippocampal formations from representative cases. The right (injected) hippocampal formations in control rats injected with saline (A1-4) and the left (uninjected) hippocampal formations in rats treated with MSO (B1-4) appear normal by visual examination. **I.e. there are** intact neurons in the dentate hilus, unremarkable pyramidal cell layers in CA3 and CA1 (arrows in A2-4, B2-4) and normal glial cell densities (arrowheads in A2-4, B2-4). In contrast, right hippocampal formations injected with MSO **often** exhibit classic hippocampal sclerosis characterized by a shrunken hippocampus (C1), reactive gliosis (arrowheads in C2-4) and neuron loss primarily in the dentate hilus, CA3 and CA1 (asterisks in C2, 3 and 4, respectively). Some hippocampal formations injected with MSO also exhibit degeneration of neurons in the dentate granular cell layer (upper asterisks in C2). Compared to specimens from sham-operated control rats (D1-4), hippocampal formations from rats stimulated for 3 h (E1-4) or 8 h (F1-4) displayed hippocampal pathologies that were often similar to end-folium sclerosis or hippocampal sclerosis. Severe neuron loss (asterisks in E2, F2) and reactive gliosis (arrowheads in E2, F2) were seen in the dentate hilus after both stimulation protocols, **similar to end-folium sclerosis**. Loss of pyramidal neurons in CA3 and CA1, **similar to hippocampal sclerosis**, was particularly evident in the 8-h stimulation model (asterisks in F3 and 4, respectively), though significant thinning of the pyramidal cell layer was also visible in the 3-h model (asterisks in E3 and 4, respectively). Extensive reactive gliosis was found in the CA3 and CA1 areas in both the 3-h (arrowheads in E3, 4) and 8-h (arrowheads in F3, 4) models. Abbreviations: 3h and 8h STIM, hippocampal formations from rats stimulated for 3 and 8 h, respectively; CA3, CA1, subfields of hippocampus; MSO L, uninjected left hippocampal formation from rat injected with MSO into the right hippocampal formation; MSO R, right hippocampal formation injected with MSO; Saline, right hippocampal formation from control rat injected with saline; Sham-control, right hippocampal formation from sham-operated control rat. Bars: A1 through F1, 500 μm; A2-4 through F2-4, 200 μm.

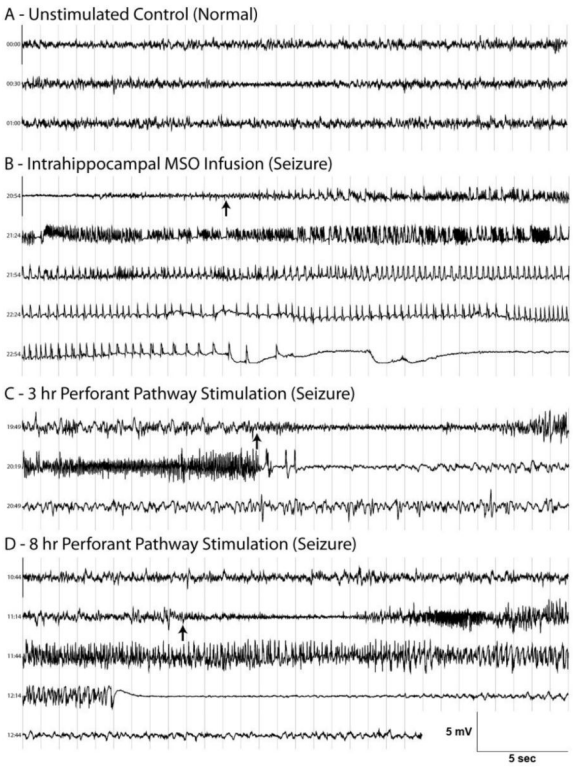

Fig. 2.

Representative traces of **continuous** intracranial EEG **recordings** from normal (A) and epileptic (B - D) rats. EEG traces were recorded from depth electrodes in either the left or right hippocampal formation (A, C and D) and from an epidural screw electrode placed over the right parietal cortex (B). All seizures shown were of Racine Stage III or higher and captured at least 3 days after seizure induction by MSO (B) or electrical stimulation (C, D). Each horizontal trace shows 30-s **of** EEG and consecutive traces are plotted in sequential order. The light-gray vertical lines demarcate 1-s time intervals, and the *Y* axis in each panel corresponds to 5 mV (±2.5 mV). Seizure onsets and offsets are marked with arrows and arrowheads, respectively.

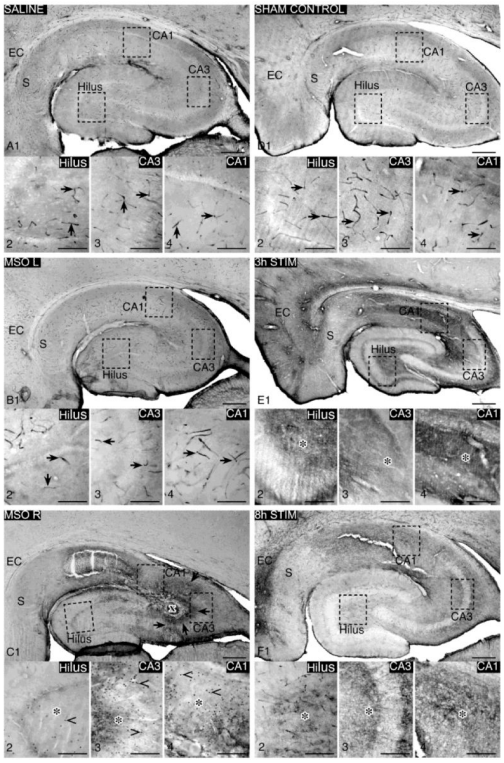

Fig. 3.

Immunohistochemistry of MCT1 on horizontal sections from representative hippocampal formations in control and MSO-treated rats. MCT1 is present on microvessels throughout the hippocampal formation in saline control rats (A1 and arrows in A2-4) and in sham-operated rats (D1 and arrows in D2-4). A similar pattern is seen in untreated left hippocampal formations in MSO-injected rats (B1 and arrows in B2-4). In the right hippocampal formation of rats injected with MSO (C1-4), MCT1 labeling is lost on microvessels in the hilus, CA3 and CA1 (asterisks in C2-4, respectively). Reduced microvascular labeling of MCT1 is also seen in the subiculum and entorhinal cortex (S and EC, respectively, in C1). Dense granular labeling with MCT1 is found diffusely around the MSO injection site (x in C1) and in parts of CA3 and CA1 (arrows in C1) in the MSO-treated right hippocampal formation. **Round, dense cells** are labeled with MCT1 and seen in close proximity to the injection site (arrowheads in C2-4) in the MSO-treated right hippocampal formation. MCT1 is lost on microvessels in the dentate hilus, CA3 and CA1 in hippocampal formations from rats stimulated for 3 h (E1-4) or 8 h (F1-4), respectively. In these rats, MCT1 labeling on microvessels is replaced by granular and dense MCT1 labeling present diffusely throughout the neuropil (E2-4, F2-4). Granular MCT1 labeling is particularly evident in areas with reactive gliosis on Nissl sections, such as the dentate hilus, CA3 and CA1 (asterisks in E2-4 and F2-4, respectively). Bars: A1 through F1, 500 μm; A2-4 through F2-4, 200 μm.

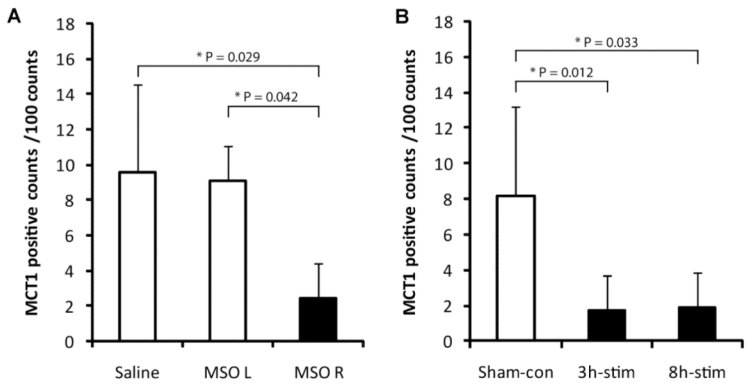

Fig. 4.

Quantitation and statistical analysis of MCT1-positive microvessels. (A) The density of MCT1-positive microvessels (expressed as the fraction of MCT1 positive counts per 100 total counts) is significantly reduced in the right hippocampal formation infused with MSO (MSO R) compared to the contralateral left (non-infused) hippocampal formation (MSO L, *$P < 0.05$), and to the saline-infused (control) hippocampal formation (Saline, $P < 0.05$). (B) The density of MCT1-positive microvessels is also significantly reduced in the hippocampal formations in the 3hr stimulated (stim) and 8hr stimulated (stim) rats vs. the non-stimulated control rats (Sham-con, *$P < 0.05$).

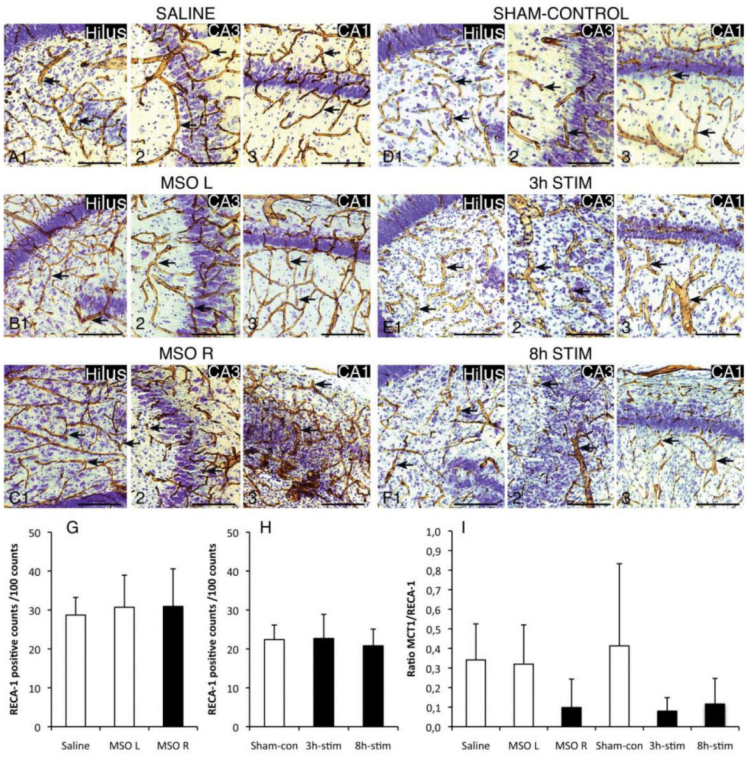

Fig. 5.

Immunohistochemistry, quantitation and statistical analysis of RECA-1-positive microvessels. RECA-1 is present on a network of microvessels that extends throughout the hippocampal subfields in all control (A, B, D) and experimental (C, E, F) rats. Visual examination did not reveal any striking reduction in RECA-1-labeling in areas of neuronal loss and reactive gliosis, such as the dentate hilus, CA3 and CA1, in either MSO R (C), 3h-stim (E) or 8h-stim (F) rats when compared to saline (A), untreated MSO L (B) or sham control (D) rats. These assessments were confirmed by quantitative analysis, which showed no change in the density of RECA-1-positive blood vessels in the hippocampal formations among saline, MSO L and MSO R rats (G) and among sham-control, 3h-stim and 8h-stim rats (H). The ratios of MCT1-positive to RECA-1-positive blood vessels were reduced in the hippocampal formations in MSO R vs. saline and MSO L rats and in 3hr-stim and 8hr-stim vs. Sham-con rats (I), although this reduction was not statistically significant. Bars: 200 μm.

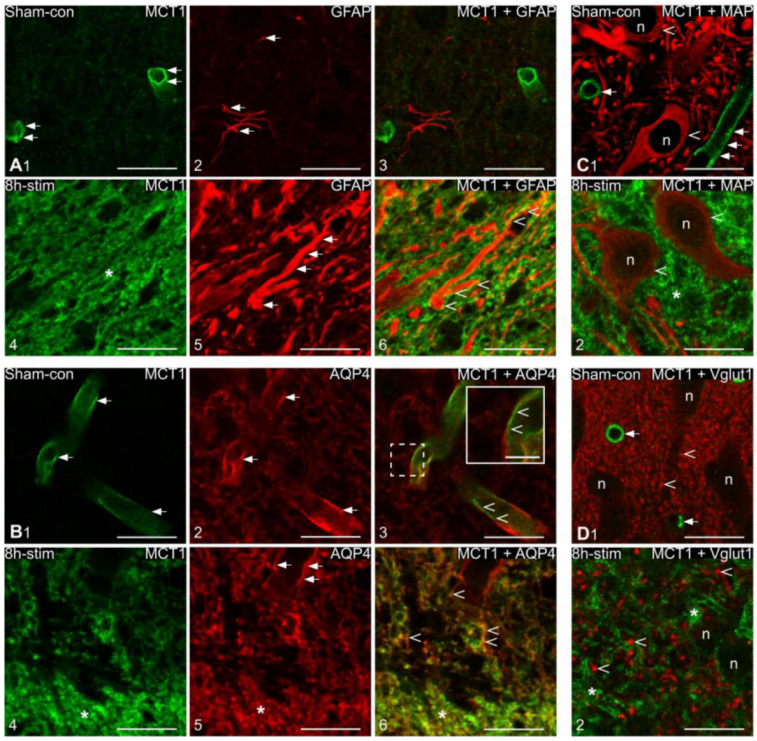

Fig. 6.

Horizontal sections of representative hippocampal formations from sham-operated control rats (Sham-con) and 8 h stimulated rats (8h-stim). The hippocampal formations are double-labeled with MCT1 and markers for astrocytes (GFAP and AQP4) and neurons (MAP and Vglut1). (A) There is abundant expression of MCT-1-positive microvessels (arrows in A_1) and GFAP-positive astrocytes (arrows in A_2) throughout the hippocampal formation in control rats. MCT1 and GFAP do *not* co-localize in these animals (A_3). There is marked up-regulation of MCT1 in the extravascular neuropil in sclerotic areas in the 8 h stimulated rats (asterisk in A_4). Reactive gliosis is also present in the same areas as visualized by intense labeling of GFAP in astrocyte processes (arrows in A_5). MCT1 and GFAP co-localize in the 8 h stimulated rats, specifically at the plasma membrane of astrocytes (yellow overlay, arrowheads in A_6). (B) There is abundant expression of MCT-1-positive (arrows in B_1) and AQP4-positive (arrows in B_2) microvessels throughout the hippocampal formation in control rats. MCT1 and AQP4 are closely associated, but they do *not* co-localize in these animals (arrowhead and inset in B_3). There is marked up-regulation of MCT1 (asterisk in B_4) and of AQP4 (asterisk and arrows in B_5) in the extravascular neuropil in sclerotic areas in the 8 h stimulated rats. MCT1 and AQP4 co-localize in the extravascular neuropil in the 8 h stimulated rats (yellow overlay, asterisks and arrowheads in B_6). (C) MAP (red) labels pyramidal cell bodies (*n*), dendrites and axons in both control (arrowheads in C_1) and 8 h stimulated rats (arrowheads in C_2). MCT1 (green; arrows in C_1 and asterisk in C_2) and MAP do not co-localize in either controls (C_1) or stimulated rats (C_2). (D) Vglut1 (red) densely labels nerve terminals (arrowheads in D_1) in control rats, while pyramidal cell bodies (*n* in D_1) are unlabeled. The dense nerve terminal labeling on each side of the pyramidal cell layer seen in the controls is replaced by scattered labeling of terminals in the pyramidal cell layer in the 8 h stimulated rats (arrowheads in D_2). Vglut1 and MCT1 (green; arrows in D_1 and asterisks in D_2) do not co-localize in controls or 8 h stimulated rats. Abbreviation: *n*, neuronal cell body. Bars, 20 μm; inset in B_3, 5 μm.

Table 1

Animal Characteristics

Model	Rat	**Days monitored by icEEG	Recurrent seizures	Neuropathology	MCT1 labeling							
					Microvessels				Granular on astrocytes			
					Hilus	CA3	CA1	Sub	Hilus	CA3	CA1	Sub
Saline control	1	13	−	Normal	++	++	++	++	0	0	0	0
	2	16	−	Lesion from cannula in dentate mol.layer	++	++	++	+	0	0	0	0
	3	14	−	Lesion from cannula in dentate hilus	+	++	++	++	0	0	0	0
	4	24	−	Lesion from cannula in dentate hilus	++	++	++	++	0	0	0	0
	5	27	−	Lesion from cannula in dentate hilus	+	++	++	++	0	0	0	0
	6	25	−	Lesion from cannula in dentate mol.layer	+	++	++	+	0	0	0	0
MSO	1	22	+	Reactive gliosis	0	+	+	++	+	+	+	0
	2	23	+	Reactive gliosis	+	++	++	++	+	0	0	0
	3	23	+	Reactive gliosis	0	0	0	0	+	+	+	0
	4	10	+	Hippocampal sclerosis (hilus, CA3, CA1)	0	0	0	0	+	+	++	+
	5	30	+	Hippocampal sclerosis (hilus, CA3, CA1)	+	0	0	++	+	++	++	0
	6	13	+	Hippocampal sclerosis (hilus, CA3, CA1)	+	0	0	++	+	+	++	0
Sham control	1	32	−	Normal	++	++	++	++	0	0	0	0
	2	37	−	Normal	++	++	++	+	0	0	0	0
	3	73	−	Normal	++	++	++	++	0	0	0	0
	4	49	−	Normal	+	+	+	+	0	0	0	0
	5	0	−	Normal	++	++	++	++	0	0	0	0
3h-stim	1	4	+	Normal	+	+	++	+	0	0	0	0
	2	16	+	Normal	+	++	++	+	+	0	0	0
	3	17	+	Normal	++	++	++		0	+	0	0
	4	45	+	Hippocampal sclerosis (hilus)	0	+	+	+	++	0	0	0
	5	59	+	Hippocampal sclerosis (hilus, CA3)	0	0	0	0	++	++	+	0
	6	4	−	Hippocampal sclerosis (hilus, CA3)	+	0	0	+	0	+	+	0
	7	20	+	Hippocampal sclerosis (hilus, CA3, CA1)	0	0	0	0	++	++	++	0
	8	2	+	Hippocampal sclerosis (hilus, CA3, CA1)	+	+	++	0	+	0	0	0

Model	Rat	**Days monitored by icEEG	Recurrent seizures	Neuropathology	MCT1 labeling							
					Microvessels				Granular on astrocytes			
					Hilus	CA3	CA1	Sub	Hilus	CA3	CA1	Sub
	9	4	+	Hippocampal sclerosis (hilus, CA3, CA1)	0	0	0	0	0	+	+	0
	10	24	+	Hippocampal sclerosis (hilus, CA3, CA1)	0	0	0	0	++	++	++	0
8h-stim	1	29	+	Hippocampal sclerosis (hilus, CA3, CA1)	+	+	++	++	+	++	0	0
	2	62	+	Hippocampal sclerosis (hilus, CA3, CA1)	+	0	0	++	+	++	++	0
	3	33	+	Hippocampal sclerosis (hilus, CA3, CA1)	+	0	0	++	+	++	++	0
	4	25	+	Hippocampal sclerosis (hilus, CA3, CA1)	0	0	0	0	+	++	++	0
	5	44	+	Large lesion	N/A*	0	0	0	N/A*	+	++	0

Abbreviations: Hilus, dentate hilus; CA3-CA1, hippocampal subfields CA3 and CA1; Sub, subiculum. MCT1 labeling intensity: 0, labeling is lost or not present; +, weak labeling; ++, strong labeling.

*Parts of the section were lost.

**The days monitored by icEEG are equal to the time of euthanasia/perfusion/tissue analysis after induction of seizures.